



Article

Protective Effects of Oroxylin A on Retinal Ganglion Cells in Experimental Model of Anterior Ischemic Optic Neuropathy

Jia-Ying Chien ^{1,†} , Shu-Fang Lin ^{2,†}, Yu-Yau Chou ³ , Chi-Ying F. Huang ^{2,4,*} and Shun-Ping Huang ^{1,3,5,*}¹ Institute of Medical Sciences, Tzu Chi University, Hualien 970, Taiwan; 100712016@gms.tcu.edu.tw² Institute of Clinical Medicine, National Yang Ming Chiao Tung University, Taipei 112, Taiwan; D55051@mail.cmuhch.org.tw³ Department of Molecular Biology and Human Genetics, Tzu Chi University, Hualien 970, Taiwan; 104712123@gms.tcu.edu.tw⁴ Institute of Biopharmaceutical Sciences, National Yang Ming Chiao Tung University, Taipei 112, Taiwan⁵ Department of Ophthalmology, Taichung Tzu Chi Hospital, Taichung 472, Taiwan

* Correspondence: cyhuang5@nycu.edu.tw (C.-Y.F.H.); sphophdoc1688@gms.tcu.edu.tw (S.-P.H.); Tel.: +886-2-28267904 (C.-Y.F.H.); +886-3-8565301#2664 (S.-P.H.)

† The authors contributed equally to this work.

Abstract: Nonarteritic anterior ischemic optic neuropathy (NAION) is the most common cause of acute vision loss in older people, and there is no effective therapy. The effect of the systemic or local application of steroids for NAION patients remains controversial. Oroxylin A (OA) (5,7-dihydroxy-6-methoxyflavone) is a bioactive flavonoid extracted from *Scutellariae baicalensis* Georgi. with various beneficial effects, including anti-inflammatory and neuroprotective effects. A previous study showed that OA promotes retinal ganglion cell (RGC) survival after optic nerve (ON) crush injury. The purpose of this research was to further explore the potential actions of OA in ischemic injury in an experimental anterior ischemic optic neuropathy (rAION) rat model induced by photothrombosis. Our results show that OA efficiently attenuated ischemic injury in rats by reducing optic disc edema, the apoptotic death of retinal ganglion cells, and the infiltration of inflammatory cells. Moreover, OA significantly ameliorated the pathologic changes of demyelination, modulated microglial polarization, and preserved visual function after rAION induction. OA activated nuclear factor E2 related factor (Nrf2) signaling and its downstream antioxidant enzymes NAD(P)H:quinone oxidoreductase (NQO-1) and heme oxygenase 1 (HO-1) in the retina. We demonstrated that OA activates Nrf2 signaling, protecting retinal ganglion cells from ischemic injury, in the rAION model and could potentially be used as a therapeutic approach in ischemic optic neuropathy.

Keywords: ischemic optic neuropathy; Oroxylin A; retinal ganglion cell; microglia; Nrf2; oxidative stress; visual evoked potential (VEP); optical coherence tomography (OCT)



Citation: Chien, J.-Y.; Lin, S.-F.; Chou, Y.-Y.; Huang, C.-Y.F.; Huang, S.-P. Protective Effects of Oroxylin A on Retinal Ganglion Cells in Experimental Model of Anterior Ischemic Optic Neuropathy.

Antioxidants **2021**, *10*, 902. <https://doi.org/10.3390/antiox10060902>

Academic Editors: Adrian Gericke and Verena Prokosch

Received: 11 May 2021

Accepted: 31 May 2021

Published: 3 June 2021

Publisher's Note: MDPI stays neutral with regard to jurisdictional claims in published maps and institutional affiliations.



Copyright: © 2021 by the authors. Licensee MDPI, Basel, Switzerland. This article is an open access article distributed under the terms and conditions of the Creative Commons Attribution (CC BY) license (<https://creativecommons.org/licenses/by/4.0/>).

1. Introduction

Nonarteritic anterior ischemic optic neuropathy (NAION) is one of the most common acute optic neuropathies in the elderly population [1], and it leads to a severe loss of visual function. The pathogenesis of NAION is probably multifactorial but remains uncertain. Predisposing risk factors such as age, small cup/disc ratio, diabetes mellitus, nocturnal hypotension, hypercholesterolemia, hypertension, coronary artery disease, and obstructive sleep apnea have been linked to NAION [2–8]. There is currently no safe and effective treatment for the disease. Accumulating evidence suggests that NAION results from impaired vascular autoregulation at the optic nerve head and leads to impaired ocular homeostasis [9–11]. These factors contribute to axonal edema and compartment syndrome for the optic nerve disc, further accelerating hypoxia, increasing oxidative stress, and inducing inflammatory processes and the consequential loss of retinal ganglion cells (RGCs) [12–17].

Neuroinflammation and microglial activation have been considered the main pathogenic mechanisms in the NAION model. Previous studies demonstrated that the invasion of

extrinsic macrophages into the optic nerve (ON) triggered the release of proinflammatory cytokines or chemokines and increased intrinsic microglial activation, leading to RGC dysfunction and death in a rodent model of NAION [18–20]. Over the decades, inflammation initiated by NAION has been an important target for investigating the pathogenesis and developing potential treatments. Our previous study showed that Oroxylin A (OA), a flavonoid abundant in the extract of *Scutellariae baicalensis* Georgi., exerts anti-apoptotic and anti-inflammatory effects in an optic nerve crush model [21]. OA has been reported to suppress inflammatory responses [22,23], ameliorate oxidative stress damage [24,25], decrease cell apoptosis [26], inhibit thrombotic activities [27], and improve neurofunctions [28–31]. However, whether OA is effective in attenuating the neuroinflammation and microglial polarization induced by experimental anterior ischemic optic neuropathy remains to be elucidated. In this research, we evaluated the effects of OA on RGC survival, the integrity of visual function, neuroinflammation, and microglial polarization in an experimental anterior ischemic optic neuropathy model, and the potential underlying molecular mechanisms were investigated.

2. Materials and Methods

2.1. Animals and Study Design

Four- to six-week-old male Wistar rats (weighing 100–125 g), obtained from Bio-LASCO.Co. Taiwan, were used in this study. All the animal procedures were approved by the Institutional Animal Care and Use Committee (IACUC) at Tzu Chi University (No. 107008). The rats were divided into three groups: sham, AION induction treated with PBS, or AION treated with the subcutaneous injection of OA (15 mg/kg [21]; Alomone labs, Jerusalem, Israel) once immediately after laser induction. The experimental design and procedures are shown in Figure 1.

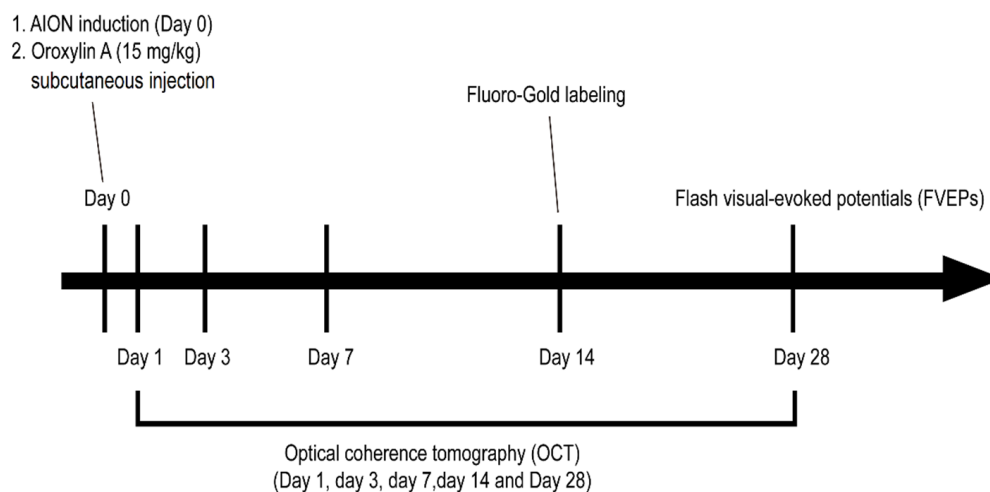


Figure 1. Schematic of the experimental design and procedures for Oroxylin A (OA) treatment in the rat anterior ischemic optic neuropathy (rAION) model.

2.2. Anesthesia and Euthanasia

We performed all the animal experiments under general anesthesia, accomplished by an intramuscular injection of a mixture of ketamine and xylazine (100 mg/kg; 10 mg/kg body weight) [14]. The animals were kept warm on a heating pad throughout whole procedure and closely monitored until full recovery. Eye drops of 0.5% Alcaine (Alcon, Puurs, Belgium) were applied topically for local anesthesia. The pupils were dilated with Mydrin-P (Santen, Osaka, Japan) in all the animal procedures. The rats were euthanized with CO₂ at a fill rate of 20% of the existing chamber volume per minute (5 L/min). Every effort was made to minimize distress and suffering in the animals.

2.3. *rAION Induction*

After general anesthesia, we performed AION induction via photodynamic thrombosis with an injection of 2.5 mM rose bengal (Sigma-Aldrich, St. Louis, MO, USA) (1 mL/Kg animal weight) in pH 7.4 phosphate buffered saline (PBS) [14,32]. Immediately after tail vein injection of rose bengal, the optic disc was exposed to an argon green laser (532 nm wavelength, 500 mm size, and 80 mW power) (MC-500 multicolor laser, Nidek Co., Ltd., Tokyo, Japan) at one sec/pulse for 12 sec pulses, each with a fundus contact lens. Tobradex eye ointment (Alcon, Fort Worth, TX, USA) was applied after the laser induction procedure. The rats were monitored daily for general physical health.

2.4. *Flash Visual Evoked Potential (FVEP)*

The FVEPs were measured at 28 days after rAION induction in 18 experimental rats using a visual electrodiagnostic system (Espion, Diagnosys LLC, Gaithersburg, MA, USA) as previously described [14,33]. We masked the groups in assessing the FVEP. The P1–N2 amplitude in each group was analyzed for visual function ($n = 6$ per group).

2.5. *Retrograde Labeling of RGCs by Fluoro-Gold (FG)*

The retrograde labeling procedures were described in detail in our previous reports [14]. Briefly, the RGC density of the retina was calculated at distances of 1 mm (central area) and 3 mm (mid-peripheral area) from the center of the optic disc. At least 10 randomly chosen areas ($38,250 \text{ mm}^2$; $225 \text{ by } 170 \text{ mm}^2$) in the central and mid-peripheral regions of each retina ($n = 6$ rats for each group) were counted.

2.6. *Immunohistochemistry (IHC)*

The frozen sections of ONs and retina were rinsed with PBS and then blocked with 5% normal goat serum containing 1% bovine serum albumin (BSA) for 30 min. The ON sections were labeled with anti-ED1 (CD68; 1:50; Bio-Rad, Berkeley, CA, USA), anti-2', 3'-cyclic nucleotide 3'-phosphodiesterase (CNPase) (1:200; Abcam, Cambridge, UK), and anti-Ym1 (1:50; Abcam) primary antibodies, and the retinal sections were labeled with anti-ionized calcium binding adaptor molecule 1 (Iba1) (1:200; Abcam) and anti-interleukin 6 (IL-6) (1:1000; Abcam) primary antibodies. Those sections were then incubated with corresponding Alexa Fluor conjugated secondary antibodies. Photographs were taken using a Zeiss LSM 900 confocal system (Carl Zeiss, Oberkochen, Germany). At least six images per eye by $20\times$ magnification were taken for quantification the ED-1 or Ym1 staining positive cell in the optic nerve and for quantification of Iba1 and IL-6 staining in the retina. To quantify the intensity of CNPase staining in optic nerve, we opened CNPase and DAPI channel in ImageJ, the intensity of CNPase and DAPI in optic nerve were measured and the CNPase generated per DAPI-positive cells were calculated.

2.7. *Fluorescent Terminal Deoxynucleotidyl Transferase dUTP Nick end Labeling (TUNEL) Staining*

Apoptotic cells in the ganglion cell layer (GCL) of the retina were detected by a TUNEL assay according to the manufacturer's protocol (DeadEnd™ Fluorometric TUNEL System; Promega Corporation, Madison, WI, USA) as described previously [4–7]. Six retina sections of each eyeball were examined using a fluorescent microscope (Zeiss), and the TUNEL-positive cells in the GCL were manually counted ($n = 6$ rats for each group).

2.8. *In Vivo Optical Coherence Tomography (OCT) Imaging*

The optic disc width and retinal nerve fiber layer (RNFL) thickness were evaluated using a Phoenix Micron IV retinal microscope with an image-guided OCT system as previously described [14,32]. We standardized the measurement by one person handled the animal and picked up the animal randomly from each group to the other person performed the OCT without knowing the animals belong to which group. The images were taken pre-rAION (Day 0) and on Days 1, 3, 7, 14, and 28 post-rAION. At least 6 clear photos

were captured for each eye at different time points. The profiles of the optic disc width and RNFL thickness were analyzed using GraphPad Prism 7.0 (GraphPad Software, La Jolla, CA, USA).

2.9. Western Immunoblotting

The experimental procedures for immunoblotting were described in detail for previous studies [14,34]. Briefly, 30 µg of retinal extracts was separated by 10% SDS-PAGE, transferred to a PVDF membrane, blocked with 5% nonfat milk, and then incubated with anti-Nrf2 (1:200; Santa Cruz, Dallas, TX, USA), anti-NQO-1 (1:200; Abcam), anti-HO-1 (1:200; NOVUS, Centennial, CO, USA), anti-Iba1 (1:500 Abcam), anti-transforming growth factor-β (TGF-β) (1:500; Cell Signaling Technology, Danvers, MA, USA), and anti-GAPDH (1:3000; Sigma-Aldrich, St. Louis, MO, USA) primary antibodies. The blots were washed and incubated with corresponding secondary antibodies (1:10,000; Bio-Rad). The positive protein bands on the blot were detected using ECL kits (RPN2232, GE Healthcare, Piscataway, NJ, USA) and exposed using a BioSpectrum® Imaging System (UVP BioSpectrum 810, UK). The signal intensity was measured and analyzed using ImageJ 1.8.0_172 (U.S. National Institutes of Health, Bethesda, Maryland, USA, <https://imagej.nih.gov/ij/>, accessed on 28 May 2021).

2.10. Statistical Analysis

All the data are presented as the mean ± standard deviation (SD). Statistical analysis was performed using the Mann-Whitney U test and the Kruskal-Wallis test for comparisons between groups via GraphPad Prism 7 (GraphPad Software, La Jolla, CA, USA). *p*-values less than 0.05 were considered to indicate statistical significance.

3. Results

3.1. OA Promoted Retinal Ganglion Cell Survival

The fluoro-gold (FG) retrograde labeling of RGCs was performed to determine the neuroprotective effect of OA on the RGCs after infarction. The mean RGC counts in the central retina in the sham, PBS-treated, and OA-treated groups were 2056 ± 361, 538 ± 144, and 1315 ± 490 cells/mm², respectively (Figure 2A–C,G). The mean RGC counts in the mid-peripheral retina in the sham, PBS-treated, and OA-treated groups were 1294 ± 377, 487 ± 274, and 847 ± 400 cells/mm², respectively (Figure 2D–F,H). The RGC survival rates after OA treatment were increased by 37.79% in the central retina and 26.82% in the mid-peripheral retina compared with those for the PBS-treated group. OA treatment significantly increased RGC survival after ischemic injury.

3.2. OA Preserved Visual Function after AION Induction

To determine the visual function, the P1–N2 amplitudes in the flash visual evoked potentials (FVEPs) were recorded 28 days after the ischemic injury in each group. The average P1–N2 amplitudes in the sham, PBS-treated, and OA-treated groups were 44.34 ± 8.05, 16.3 ± 6.32, and 42.56 ± 10.91 µV, respectively (Figure 3). Significantly higher P1–N2 amplitude in the OA-treated group compared with that in the PBS-treated group was observed. The data indicate that the administration of OA can preserve visual function after ischemic injury.

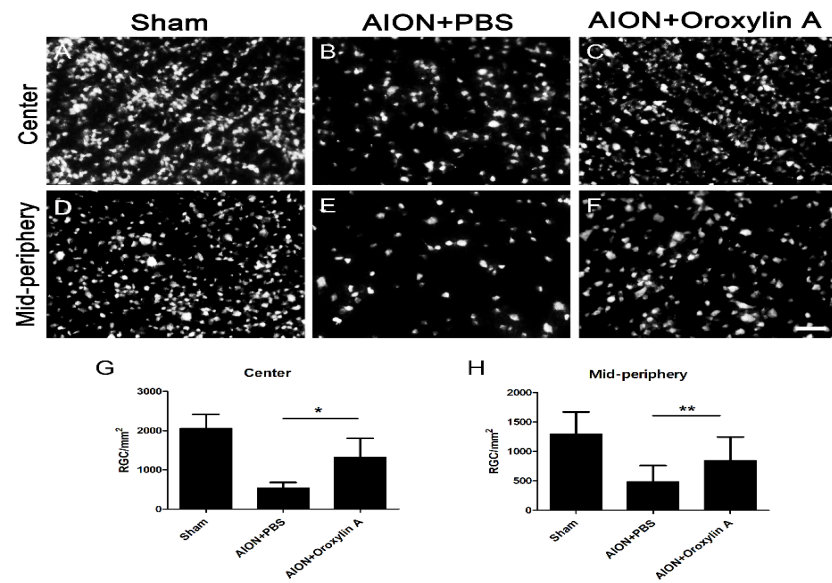


Figure 2. Effect of OA on the preservation of retinal ganglion cells (RGCs) after rAION. Representative images of RGC density in the retinal whole mount after rAION in each group (A–F). The RGC density of the OA-treated group was markedly higher than that of the PBS-treated group in the (G) central (1315 ± 490 versus 538 ± 144 cells/mm², respectively) and (H) mid-peripheral retina (847 ± 400 versus 487 ± 274 cells/mm², respectively). Results represent the means \pm SDs. Scale bar, 50 μ m; * $p \leq 0.05$, ** $p \leq 0.01$; $n = 6$.

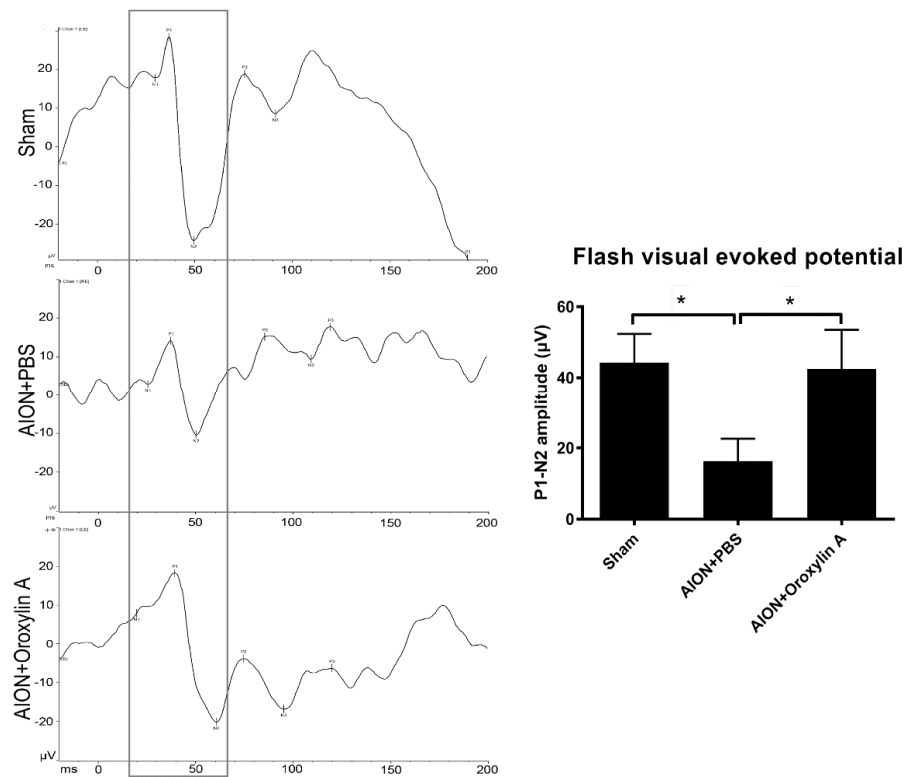


Figure 3. Effects of OA on visual function. Representative flash visual evoked potential (FVEP) at 4 weeks after rAION induction. The bar charts show the P1–N2 amplitudes of FVEP. The sham and OA-treated groups showed significantly higher P1–N2 amplitudes than the PBS-treated group (42.56 ± 10.91 μ V versus 16.3 ± 6.32 μ V, respectively). Results represent the means \pm SDs. * $p \leq 0.05$; $n = 6$.

3.3. OA Alleviated Optic Disc Swelling and Maintained RNFL Thickness after rAION Induction

The optic nerve width (ONW) profiles of the sham, PBS-treated, and OA-treated groups were recorded on Days 1, 3, 7, 14, and 28 (Figure 4). At the acute stage of rAION, macrophage infiltration causes immediate ON edema after ischemic insult; severe edema was observed on Day 1 and had been resolved on Day 7. The spectral-domain OCT was used to quantitatively monitor changes in the ONW over time. There was a significant alleviation in ON edema in the OA-treated group compared with the PBS-treated group on Days 7, 14, and 28. The OCT profiles of the RNFL thickness measurements for the sham, PBS-treated, and OA-treated groups were determined on Days 1, 3, 7, 14, and 28 (Figure 5). Compared with the PBS-treated group, the OA-treated group exhibited significant preservation of the RNFL on Day 28.

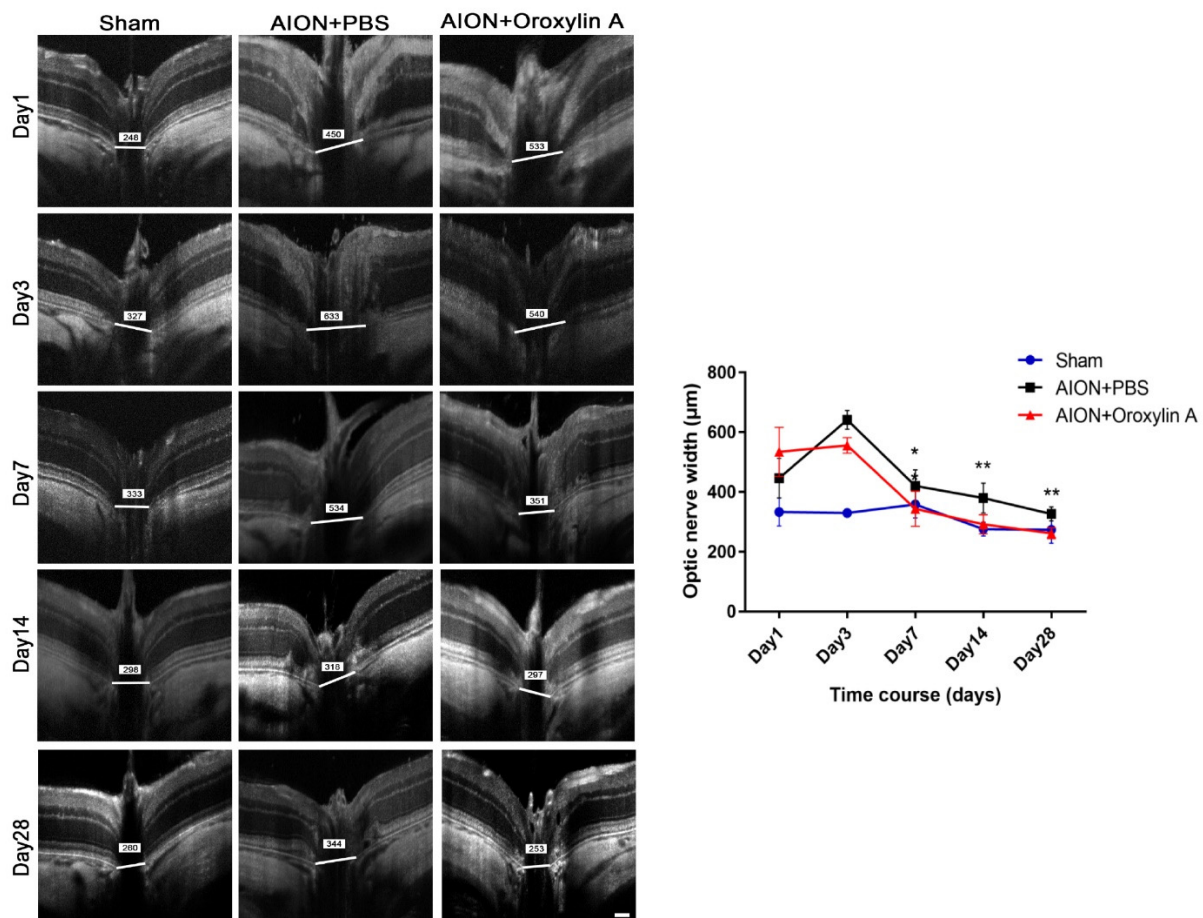


Figure 4. Optical coherence tomography (OCT) profiles of the optic nerve width (ONW). Representative ONW profiles for the sham, PBS-treated, and OA-treated groups on Days 1, 3, 7, 14, and 28. The ONW profile over time. The OA-treated group exhibited a significant reduction in edema on Days 7, 14, and 28 compared with the PBS-treated group. ($420.73 \pm 53.67 \mu\text{m}$ versus $344.11 \pm 59.01 \mu\text{m}$; $380.33 \pm 49.90 \mu\text{m}$ versus $292.60 \pm 31.95 \mu\text{m}$; and $326.92 \pm 23.26 \mu\text{m}$ versus $262.42 \pm 17.96 \mu\text{m}$, respectively). Results represent the means \pm SDs. Scale bar, $130 \mu\text{m}$; ** $p < 0.01$; * $p < 0.05$; $n = 6$.

3.4. OA Decreased RGC Apoptosis Induced by rAION

In situ TUNEL assay on retinal cross sections was performed to evaluate whether OA can protect RGCs from apoptosis (Figure 6). The numbers of TUNEL+ cells in the sham, PBS-treated, and OA-treated groups were 2.1 ± 1.1 , 20.7 ± 3.9 , and 10.6 ± 2.4 cells/high power field (HPF), respectively. The OA-treated group showed significantly less TUNEL+ cells than the PBS-treated group in the retina.

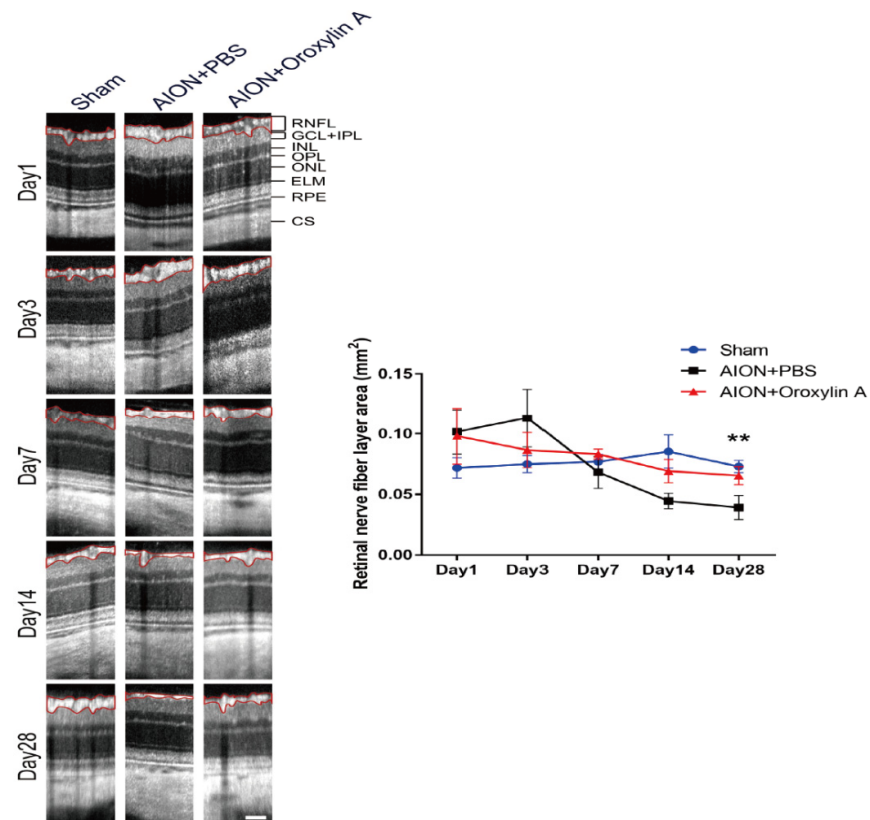


Figure 5. OCT profiles of the retinal nerve fiber layer (RNFL). Representative RNFL thickness measurements for the sham, PBS-treated, and OA-treated groups on Days 1, 3, 7, 14, and 28. Compared with the PBS-treated group, the OA-treated group exhibited significant preservation of the RNFL on Day 28 after infarction. ($0.039 \pm 0.001 \text{ mm}^2$ versus $0.065 \pm 0.0074 \text{ mm}^2$, respectively). Results represent the means \pm SDs. Scale bar, $130 \mu\text{m}$; $** p < 0.01$; $n = 6$. RNFL: retinal nerve fiber layer; GCL + IPL: ganglion cell layer + inner plexiform layer; INL: inner nuclear layer; OPL: outer plexiform layer; ONL: outer nuclear layer; ELM: external limiting membrane; RPE: retinal pigment epithelium; CS: choroidal stroma.

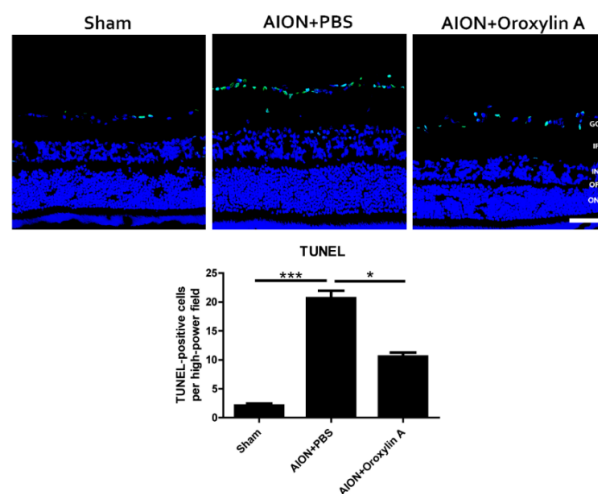


Figure 6. TUNEL assay in the retinal sections after rAION in each group. After ischemic injury, rats treated with OA showed significantly less TUNEL+ cells (green) than rats treated with PBS (10.6 ± 2.4 versus 20.7 ± 3.9 cells/HPF, respectively). Results represent the means \pm SDs. Scale bar, $50 \mu\text{m}$; $* p < 0.05$, $*** p < 0.001$; $n = 6$. GCL: ganglion cell layer; IPL: inner plexiform layer; INL: inner nuclear layer; OPL: outer plexiform layer; ONL: outer nuclear layer.

3.5. OA Decreased Inflammatory Markers

Blood-borne macrophages (indicated by ED1, a marker of CD38, specific for extrinsic macrophages) infiltrated the ON tissue and induced tissue inflammation after rAION induction. Immunostaining for ED1 in ON tissue was performed to evaluate whether OA treatment will attenuate the extrinsic macrophage infiltration in ONs 28 days after rAION (Figure 7A,D). The numbers of ED1-positive cells per HPF in the sham group, PBS-treated group, and OA-treated group were 14.6 ± 5.2 , 97.8 ± 15.8 , and 62.6 ± 15.4 , respectively. The OA-treated group showed a significant reduction in ED1-positive cells in the ON compared with the PBS-treated group. These results suggested that OA treatment can reduce extrinsic macrophage infiltration in ON after ischemic injury.

The upregulation of ionized calcium binding adapter molecule 1 (Iba1), a microglial marker, indicates microglial activation during neuroinflammation [35,36]. The inflammation response to ischemic injury, the resting microglia is activated to M1 subtypes secreting one of the proinflammatory cytokines, IL-6. It will further promote microglia polarization to M1 phenotype and release more IL-6 [37]. We also performed immunohistochemistry for Iba1 and IL-6 in the retina 4 weeks after rAION. The bar chart reveals that the numbers of Iba1-positive cells per HPF in the sham group, PBS-treated group, and OA-treated group were 72.3 ± 34.7 , 332.4 ± 90.1 , and 103.2 ± 38.3 cells/HPF, respectively (Figure 7B,E). The numbers of IL-6-positive cells per HPF in the sham group, PBS-treated group, and OA-treated group were 46.6 ± 26.1 , 188.6 ± 43.4 , and 82.5 ± 42.5 cells/HPF, respectively (Figure 7C,F). Our data demonstrate that OA significantly attenuated the levels of the proinflammatory cytokine IL-6 and decreased activated microglia in the retina after ischemic injury.

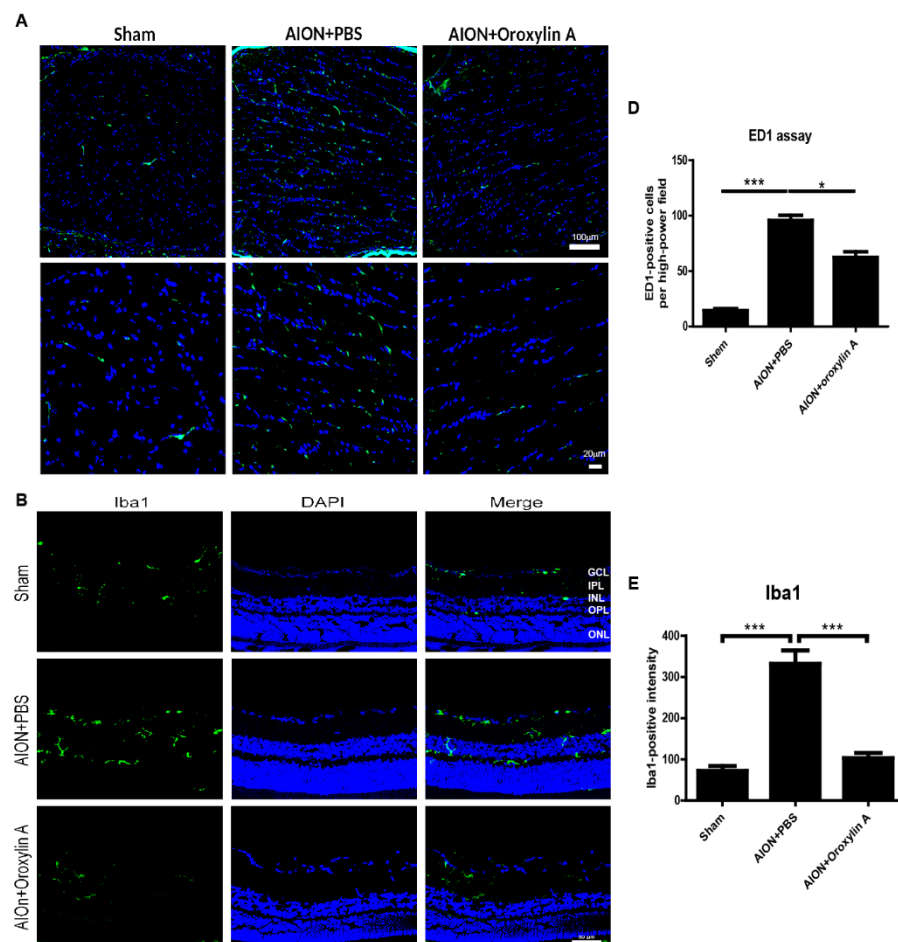


Figure 7. Cont.

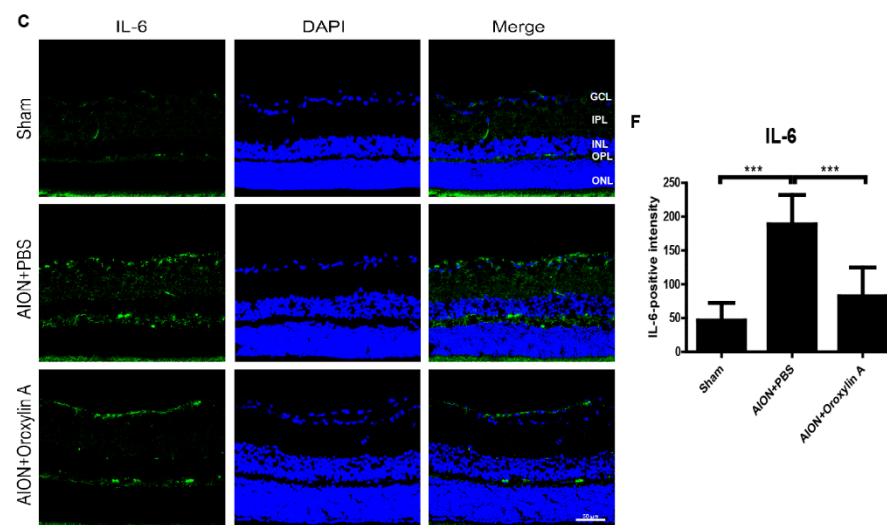


Figure 7. Immunohistochemistry (IHC) of ED1, Iba1, and IL-6 in optic nerves (ONs) 28 days after rAION. (A) the lower column indicates the ED1-positive cells (green) per HPF in the sham, PBS-treated, and OA-treated groups. (D) the OA-treated group showed significantly fewer ED1-positive cells in the ONs than did the PBS-treated group. The columns indicate that the numbers of ED1-positive cells (green) per HPF in the sham group, PBS-treated group, and OA-treated group were 14.56 ± 5.18 , 95.75 ± 15.78 , and 62.6 ± 15.39 cells/HPF, respectively. (B) immunohistochemistry of Iba1 in the retinas 4 weeks after rAION. (E) the columns indicate that the numbers of Iba1-positive cells (green) per HPF in the sham group, PBS-treated group, and OA-treated group were 72.3 ± 34.7 , 332.4 ± 90.1 , and 103.2 ± 38.3 cells/HPF, respectively. (C) immunohistochemistry of IL-6 (green) in the retinas 4 weeks after rAION. (F) the columns indicate that the numbers of IL-6-positive cells per HPF in the sham group, PBS-treated group, and OA-treated group were 46.6 ± 26.1 , 188.6 ± 43.4 , and 82.5 ± 42.5 cells/HPF, respectively. Results represent the means \pm SDs. A: Scale bar, 100 μ m (upper), 20 μ m (lower); B and C: Scale bar, 50 μ m; $n = 6$ in each group. * $p < 0.05$, *** $p \leq 0.001$. GCL: ganglion cell layer; IPL: inner plexiform layer; INL: inner nuclear layer; OPL: outer plexiform layer; ONL: outer nuclear layer.

3.6. OA Maintained the Integrity of the Myelin Sheath

2',3'-Cyclic nucleotide 3'-phosphodiesterase (CNPase) is a myelination-associated enzyme and is highly expressed in the myelin-producing oligodendrocyte cells and Schwann cells [38]. Some studies have indicated that reduced CNPase levels contribute to several neurodegenerative and demyelinating diseases [39–44]. We performed IHC of CNPase in the ONs 4 weeks after infarction to evaluate the demyelinating conditions in the optic nerve (Figure 8). CNPase was highly expressed in the optic nerve in the sham group, whereas the expression was significantly reduced after rAION induction. Furthermore, OA treatment promoted CNPase expression in the ON after infarction, suggesting that OA maintained myelin integrity in the rAION model.

3.7. Activation of Nrf2 Signaling Contributed to the Neuroprotective Effects of OA in Retina

To elucidate the molecular mechanisms involved in the neuroprotective effect of OA on RGCs, the expression of genes regulating cytoprotective responses to inflammation and oxidative stress was determined by immunoblotting analysis. We analyzed the expression of Nrf2, NQO-1, and HO-1 in the retinas after rAION. rAION induction suppressed Nrf2's expression and that of its downstream regulated genes, NQO-1 and HO-1. OA significantly enhanced the protein expression of Nrf2, NQO-1, and HO-1 in the retinas 28 days after rAION (Figure 9).

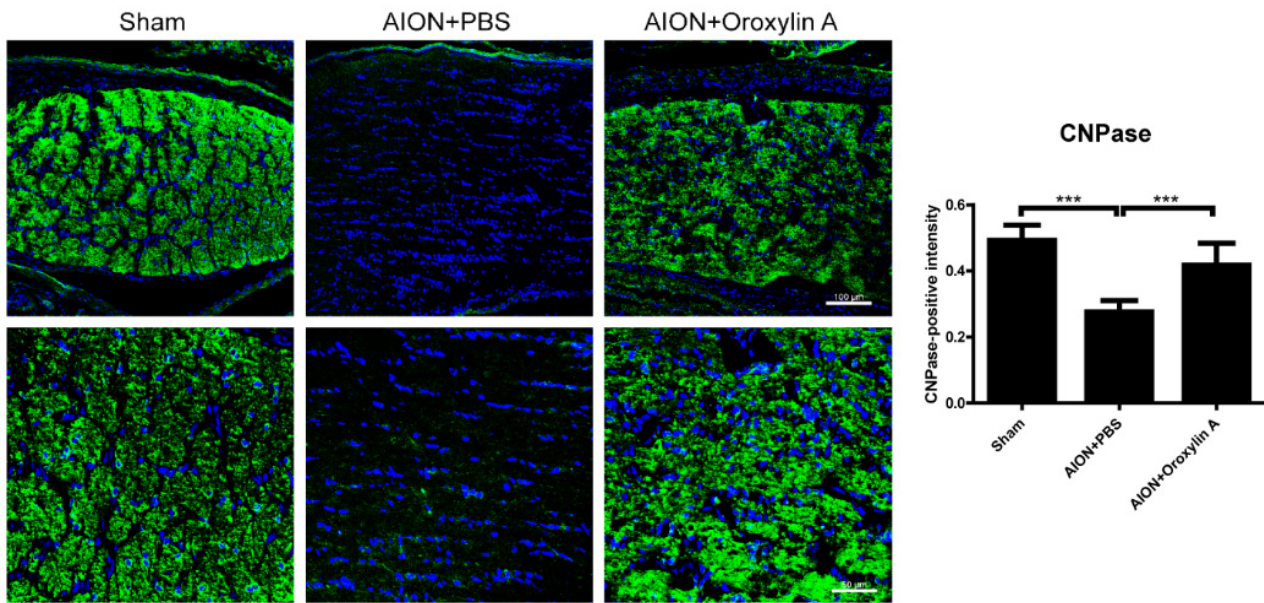


Figure 8. IHC of 2', 3'-cyclic nucleotide 3'-phosphodiesterase (CNPase) in the ON 4 weeks after rAION induction. Green fluorescence represents CNPase-positive cells, and blue fluorescence represents nuclei. The columns indicate the intensity of the green fluorescence of CNPase-positive cells. The columns indicate that the numbers of CNPase-positive intensity (green) per DAPI in the sham group, PBS-treated group, and OA-treated group were 0.49 ± 0.047 , 0.28 ± 0.035 , and 0.42 ± 0.067 intensity/DAPI, respectively. Scale bar, 100 μm (upper), 50 μm (lower); Results represent the means \pm SDs, $n = 6$ in each group. *** $p \leq 0.001$.

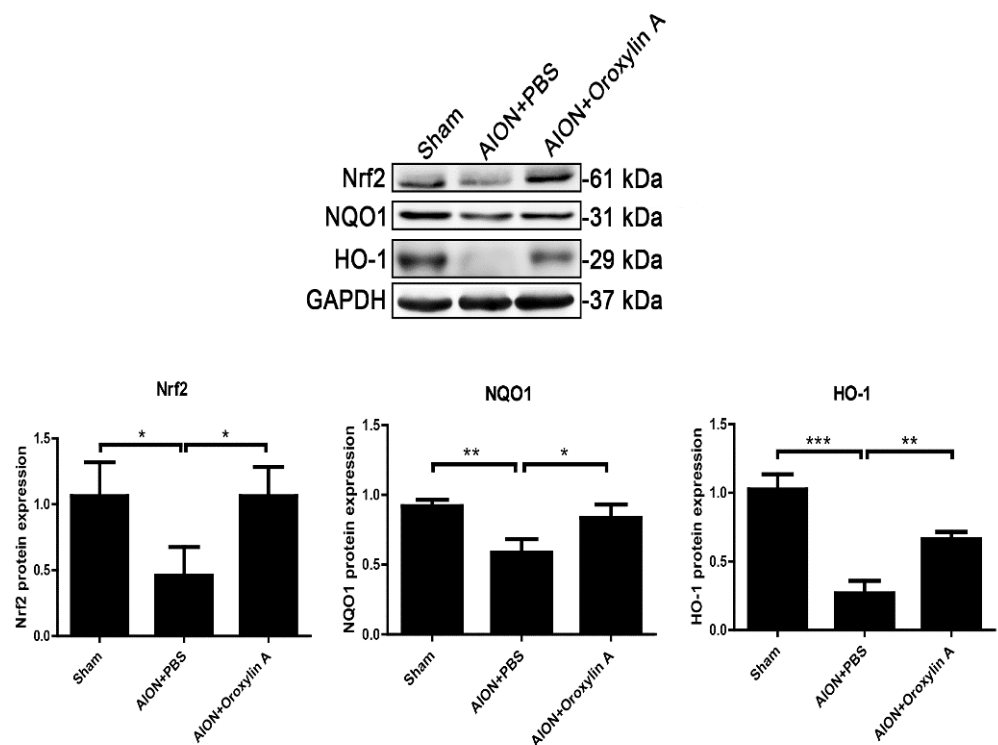


Figure 9. Immunoblotting analysis of Nrf2, NQO-1, and HO-1 protein expression levels 4 weeks after rAION. The bar graph shows that the expression levels of Nrf2, NQO-1, and HO-1 were decreased after rAION induction but significantly enhanced by treatment with OA. Results represent the means \pm SDs and are presented as ratios with the GAPDH value for three independent experiments. * $p \leq 0.05$, ** $p \leq 0.01$, *** $p \leq 0.001$.

3.8. OA Modulated Microglial Polarization

Microglia and macrophages are polarized to M1 or M2 phenotypes and mediate corresponding signaling pathways in response to different pathophysiological states [45–47]. From Figure 6, we can see that OA suppressed extrinsic macrophage invasion and decreased intrinsic microglial activation after ischemic infarction. To further evaluate whether OA would modulate microglial polarization after ischemic optic nerve injury, we examined the protein expression levels of Ym1 and TGF- β , cytokines generated by M2 microglia, and Iba1 as a microglial marker in the ON. After ischemic injury, the expression of Iba1 was dramatically enhanced in the ON, while the administration of OA significantly reduced the Iba1 level in the ON (Figure 10C,D). Furthermore, OA induced significantly more Ym1-positive cells (Figure 10A,B) and upregulated TGF- β expression in the ON after rAION induction (Figure 10C,E). These results indicate that OA-modulated microglia were polarized toward the anti-inflammatory M2 phenotype after optic nerve ischemic injury.

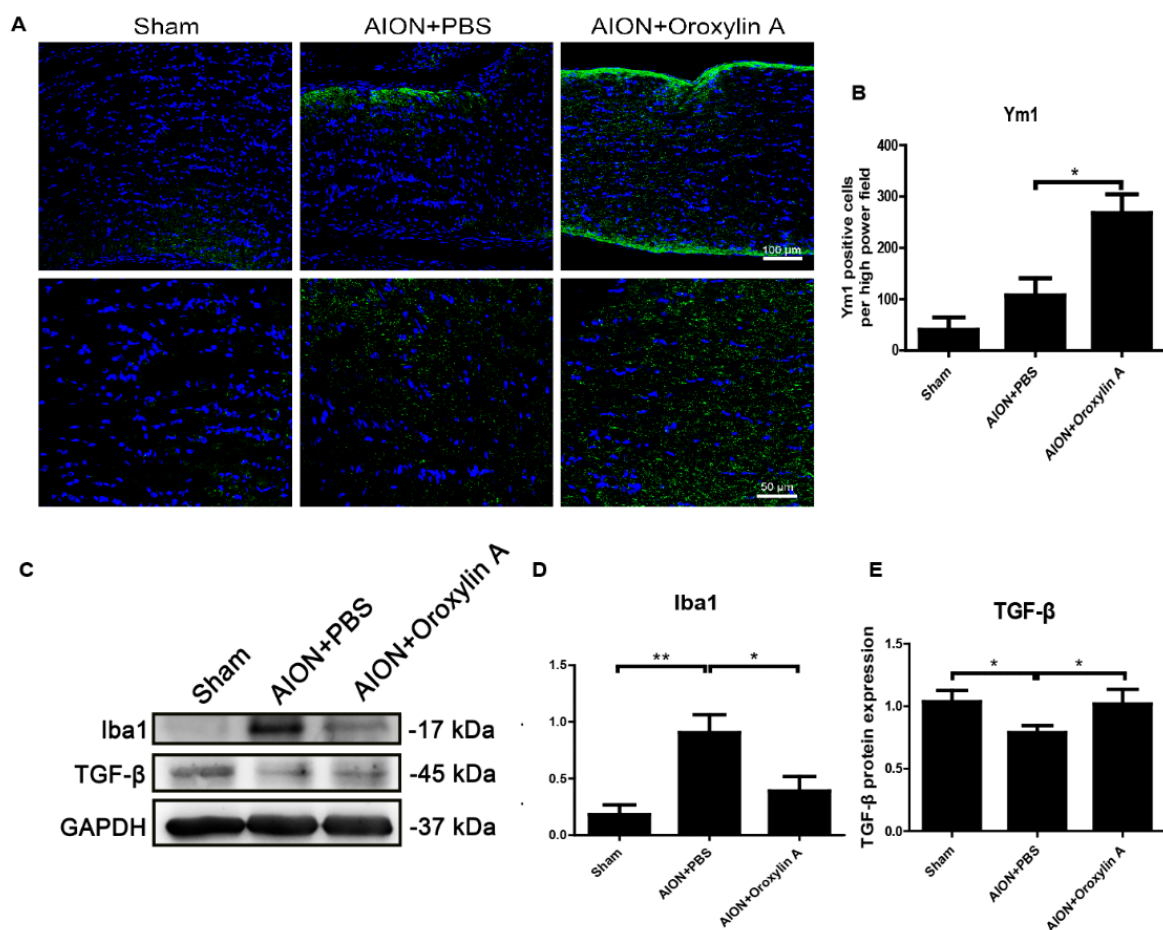


Figure 10. (A) IHC of Ym1 in the ONs 28 days after rAION. (B) the bar chart indicates that the numbers of Ym1-positive cells (green) per HPF in the sham, PBS-treated, and OA treated-groups were 40.3 ± 24.3 , 107.2 ± 33.5 , and 268 ± 36.8 , respectively. Scale bar, 50 μ m, $N = 6$ in each group. (C) immunoblotting analysis of the expression levels of Iba1 and TGF β in the ONs after rAION. OA suppressed Iba1 and increased TGF β in the ONs 28 days after rAION. (D,E) quantitative analysis of (C). Results represent the means \pm SDs and are presented as ratios with the GAPDH value for three independent experiments. Scale bar, 100 μ m (upper); 50 μ m (lower); * $p \leq 0.05$, ** $p \leq 0.01$.

4. Discussion

Our morphologic data from this study clearly show that OA treatment enhanced RGC survival and significantly reduced the recruitment of inflammatory cells into the optic nerve after infarction. Furthermore, OA not only prevented RGC apoptosis but also

preserved RGC function as demonstrated by FVEP, confirming its beneficial effect on the ischemic injury of the optic nerve. In addition, we observed that OA treatment ameliorated neuroinflammation and selectively polarized microglia toward an anti-inflammatory M2 status, resulting in a neuroprotective effect.

Post-ischemic inflammatory responses were identified in the rAION model, including the release of proinflammatory cytokines, extrinsic macrophage infiltration, intrinsic microglial activation, and the breakdown of the blood–optic nerve barrier [14,15,18,20,48]. ON ischemia triggered early inflammatory cytokine release, followed by subsequent extrinsic or intrinsic inflammatory cell invasion and activation, leading to axon dysfunction and RGC loss. Interleukin 6 (IL-6) acts as both a proinflammatory and neuropoietic cytokine involved in the development of the nervous system and neuron differentiation or degeneration. The role of IL-6 in RGC damage or protection remains controversial. Several studies have shown that a reduction in proinflammatory cytokines, including IL-6, IL-1 β , inducible nitric oxidase synthase (iNOS), and tumor necrosis factor- α (TNF- α), improves RGC survival after optic nerve injury [34,49–52]. In the present study, we found that increased IL-6 immunostaining was mainly located in the RGC layers after ischemic injury (Figure 7C,F), and OA treatment could reduce the release of IL-6, which was shown to be synthesized in damaged RGCs and to be an important marker for the disruption of axonal transport [53]. OA further attenuates rAION-induced extrinsic macrophage invasion (Figure 7A,D) and intrinsic microglia activation (Figure 7B,E). These data indicate that OA blocks early ischemia-induced inflammatory responses, leading to the alleviation of optic disc swelling and preservation of RNFL thickness (Figures 4 and 5).

Axon demyelination and/or focal damage to the ON has been identified in clinical NAION patients and NAION animal models [20,54,55]. RGC degeneration resulting from axon demyelination may be an important contributor to severe visual impairment. Direct changes in axon myelination were demonstrated by the CNPase immunostaining of the ON (Figure 8). Consistent with previous studies, we observed a markedly reduced CNPase staining of the ON after ischemic injury, and OA treatment maintained the level of CNPase staining in the infarcted ON, which indicates that OA significantly reduces ON demyelination and stabilizes the myelin sheath.

Microglia/macrophage-mediated neuroinflammation has been considered to be an important contributing factor in the pathogenesis of ischemic optic neuropathy [18–20,48]. In response to different stimuli, microglia can switch to two different phenotypes: M1 and M2. The classically activated M1 microglia, serving as the first line of defense, recognize deleterious stimuli and produce proinflammatory cytokines such as IL-1 β , IL-6, iNOS, cyclooxygenase-2 (COX2), TNF- α , several chemokines, reactive oxygen species (ROS), and other toxic molecules [56–59]. The persistent activation of M1 microglia induces chronic inflammation, accelerating neurodegenerative processes. The polarization of alternatively activated M2 microglia occurs in response to specific anti-inflammatory factors, such as IL-4, IL-10, IL-13, and TGF- β . The M2 microglia-mediated induction of IL-4, Arg1, Ym1, and TGF- β suppresses inflammation and supports neuron differentiation, the repair or regeneration of the nervous system, and the restoration of tissue homeostasis [60–63]. In this study, we found that OA treatment not only diminished ischemia-induced ED1 and Iba1 expression but further induced the expression of M2 microglia markers, Ym1 and TGF- β , in the ON after infarct injury (Figure 10). These data suggest that OA can promote microglia/macrophage polarization into M2 microglia, suppressing inflammation and facilitating recovery following ON infarction.

Oxidative stress resulting from mitochondrial dysfunction, the overproduction of ROS, and an impaired antioxidant system contributes to the pathogenesis of many ocular diseases [64–66]. The nuclear factor erythroid 2-related factor (Nrf2) signaling pathway activated by oxidative stress regulates downstream antioxidant or detoxifying enzymes, resulting in anti-inflammatory and anti-apoptotic effects [24,67–71]. Our previous report demonstrated that the activation of the Nrf2 signaling pathway protects RGCs against ischemic injury through its anti-inflammatory and anti-apoptotic actions [14]. Moreover,

recent reports indicated that the activation of Nrf2 signaling could inhibit M1-microglia-induced proinflammatory responses and polarize microglia/macrophages toward anti-inflammatory M2 microglia [72–76]. Our present data show that the Nrf2 pathway was significantly activated by OA treatment after rAION induction. These findings support the assertion that the beneficial effects of OA for ischemic optic neuropathy are associated with the activation of Nrf2 signaling, promoting M2 microglia polarization and attenuating the ischemia-induced inflammation and demyelination and apoptotic death of RGCs.

Base on the evidence from this study and our previous study [14], the data suggest activation of the Nrf2 signaling pathway promotes RGC survival and preserved the visual function after optic nerve ischemic injury. We will further evaluate effects of the Nrf2 activators, which have been used in the clinical trials for other indications, in this experimental ischemic optic neuropathy model to facilitate the translational application to NAION patients in the soon future.

5. Conclusions

In summary, this study provides evidence that OA promotes retinal ganglion cell survival and preserves visual function by preventing the apoptosis of RGCs, maintaining myelin sheath integrity, reducing the levels of proinflammatory cytokines, and modulating microglial polarization. These neuroprotective effects were achieved by the activation of Nrf2 signaling in the retina (Figure 11). Our data indicate that OA has the potential to be a future therapeutic agent for ischemic optic neuropathy.

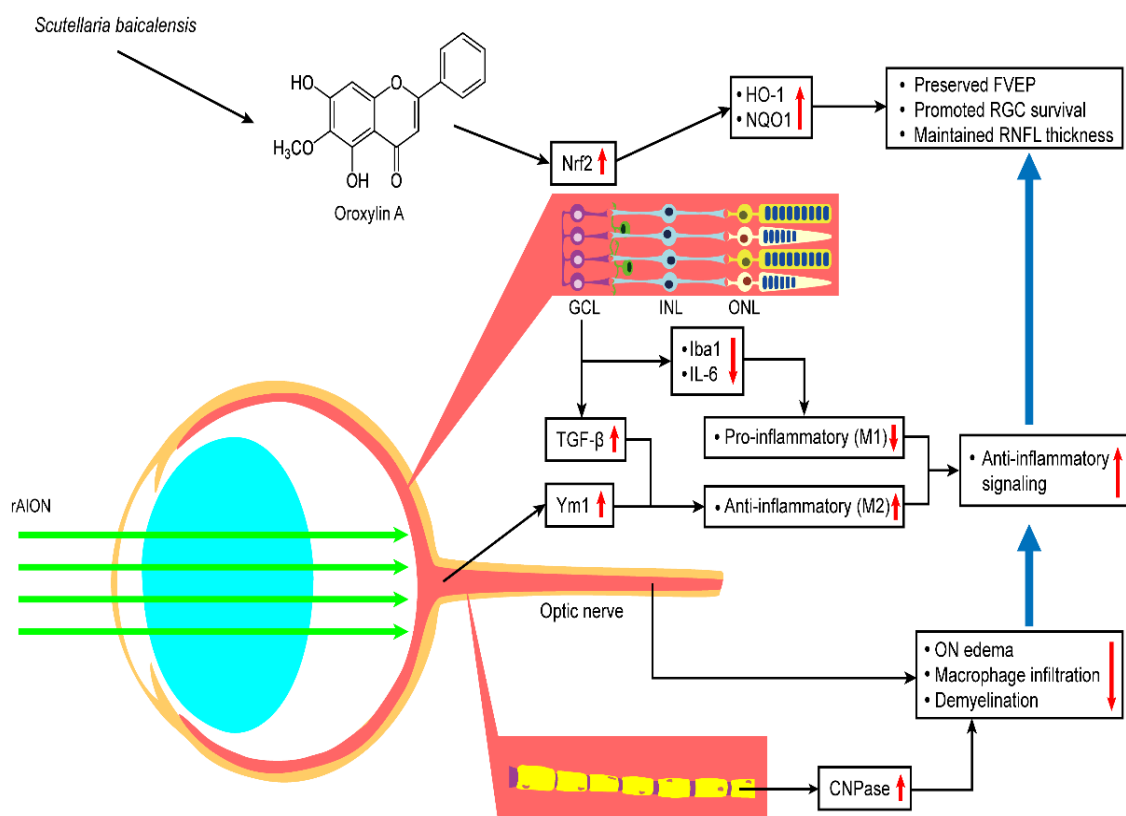


Figure 11. Hypothetical model of the protective effects of OA in the rAION model. OA treatment after rAION induction can enhance Nrf2 pathway activation and thereby preserve FVEP, promote RGC survival, and maintain RNFL thickness. OA also shows anti-inflammatory effects and modulates microglia polarization by increasing TGF- β and Ym-1 expression and decreasing Iba1 and IL-6 expression. OA protects the optic nerve by reducing ON edema, macrophage infiltration, and demyelination.

Author Contributions: Conceptualization, S.-P.H. and C.-Y.F.H.; methodology, software, validation, and formal analysis, S.-P.H., J.-Y.C., Y.-Y.C. and S.-F.L.; resources, S.-P.H.; writing—original draft preparation, S.-F.L., J.-Y.C. and S.-P.H.; writing—review and editing, S.-P.H. and C.-Y.F.H.; supervision, S.-P.H. and C.-Y.F.H.; project administration, S.-P.H.; funding acquisition, S.-P.H. and C.-Y.F.H. All authors have read and agreed to the published version of the manuscript.

Funding: This research was supported by the Ministry of Science and Technology of TAIWAN under the grant number MOST 105-2628-B-320-002-MY3 to S.-P.H. and MOST 109-2320-B-010-026- to C.-Y.F.H.

Institutional Review Board Statement: All the animal procedures carried out in this study were reviewed and approved by the Institutional Animal Care and Use Committee (IACUC) at Tzu Chi University (Approval No. 107008; 2018/03/01), Taiwan.

Informed Consent Statement: Not applicable.

Data Availability Statement: All data generated or analyzed during this study are included in this publication article.

Acknowledgments: We are grateful for the technical support from the Core Research Laboratory, Tzu Chi University, for their assistance with the Diagnosys Celeris System and confocal image analysis.

Conflicts of Interest: The authors declare no conflict of interest. The funders had no role in the design of the study; in the collection, analyses, or interpretation of data; in the writing of the manuscript; or in the decision to publish the results.

References

1. Bernstein, S.L.; Johnson, M.A.; Miller, N.R. Nonarteritic anterior ischemic optic neuropathy (NAION) and its experimental models. *Prog. Retin. Eye Res.* **2011**, *30*, 167–187. [[CrossRef](#)]
2. Hayreh, S.S.; Joos, K.M.; Podhajsky, P.A.; Long, C.R. Systemic diseases associated with nonarteritic anterior ischemic optic neuropathy. *Am. J. Ophthalmol.* **1994**, *118*, 766–780. [[CrossRef](#)]
3. Kim, M.S.; Jeong, H.Y.; Cho, K.H.; Oh, S.W.; Byun, S.J.; Woo, S.J.; Yang, H.K.; Hwang, J.M.; Park, K.H.; Kim, C.K.; et al. Nonarteritic anterior ischemic optic neuropathy is associated with cerebral small vessel disease. *PLoS ONE* **2019**, *14*, e0225322. [[CrossRef](#)] [[PubMed](#)]
4. Bandi, M.F.G.; Naserbakht, M.; Tabasi, A.; Marghaiezhadeh, A.; Esfahani, M.R.; Golzarian, Z. Obstructive sleep apnea syndrome and non-arteritic anterior ischemic optic neuropathy: A case control study. *Med. J. Islam. Repub. Iran.* **2015**, *29*, 300.
5. Cerovski, B.; Sarić, B. Risk factors in nonarteritic anterior ischemic optic neuropathy. *Acta Med. Jugosl.* **1990**, *44*, 533–540.
6. Mojon, D.S.; Hedges, T.R., 3rd; Ehrenberg, B.; Karam, E.Z.; Goldblum, D.; Abou-Chebl, A.; Gugger, M.; Mathis, J. Association between sleep apnea syndrome and nonarteritic anterior ischemic optic neuropathy. *Arch. Ophthalmol.* **2002**, *120*, 601–605. [[CrossRef](#)] [[PubMed](#)]
7. Hayreh, S.S. Role of nocturnal arterial hypotension in the development of ocular manifestations of systemic arterial hypertension. *Curr. Opin. Ophthalmol.* **1999**, *10*, 474–482. [[CrossRef](#)] [[PubMed](#)]
8. Deramo, V.A.; Sergott, R.C.; Augsburger, J.J.; Foroozan, R.; Savino, P.J.; Leone, A. Ischemic optic neuropathy as the first manifestation of elevated cholesterol levels in young patients. *Ophthalmology* **2003**, *110*, 1041–1046. [[CrossRef](#)]
9. Rootman, J.; Butler, D. Ischaemic optic neuropathy—A combined mechanism. *Br. J. Ophthalmol.* **1980**, *64*, 826–831. [[CrossRef](#)]
10. Riva, C.E.; Hero, M.; Titze, P.; Petrig, B. Autoregulation of human optic nerve head blood flow in response to acute changes in ocular perfusion pressure. *Graefes Arch. Clin. Exp. Ophthalmol.* **1997**, *235*, 618–626. [[CrossRef](#)]
11. Collignon-Robe, N.J.; Feke, G.T.; Rizzo, J.F. Optic nerve head circulation in nonarteritic anterior ischemic optic neuropathy and optic neuritis. *Ophthalmology* **2004**, *111*, 1663–1672. [[CrossRef](#)] [[PubMed](#)]
12. Khalilpour, S.; Latifi, S.; Behnammanesh, G.; Majid, A.M.S.A.; Majid, A.S.A.; Tamayol, A. Ischemic optic neuropathy as a model of neurodegenerative disorder: A review of pathogenic mechanism of axonal degeneration and the role of neuroprotection. *J. Neurol. Sci.* **2017**, *375*, 430–441. [[CrossRef](#)] [[PubMed](#)]
13. Birer, S.; Arda, H.; Kilic, D.; Baskol, G. Systemic oxidative stress in non-arteritic anterior ischemic optic neuropathy. *Eye* **2019**, *33*, 1140–1144. [[CrossRef](#)]
14. Kapupara, K.; Wen, Y.-T.; Tsai, R.-K.; Huang, S.-P. Soluble P-selectin promotes retinal ganglion cell survival through activation of Nrf2 signaling after ischemia injury. *Cell Death Dis.* **2017**, *8*, e3172. [[CrossRef](#)]
15. Mehrabian, Z.; Guo, Y.; Weinreich, D.; Bernstein, S.L. Oligodendrocyte death, neuroinflammation, and the effects of minocycline in a rodent model of nonarteritic anterior ischemic optic neuropathy (rNAION). *Mol. Vis.* **2017**, *23*, 963–976.
16. Goldenberg-Cohen, N.; Guo, Y.; Margolis, F.; Cohen, Y.; Miller, N.R.; Bernstein, S.L. Oligodendrocyte Dysfunction after Induction of Experimental Anterior Optic Nerve Ischemia. *Investig. Ophthalmol. Vis. Sci.* **2005**, *46*, 2716–2725. [[CrossRef](#)] [[PubMed](#)]
17. Koçak, N.; Eraydın, B.; Turunç, M.; Yeter, V.; Güngör, I. Serum Inflammatory Biomarkers in Patients with Nonarteritic Anterior Ischemic Optic Neuropathy. *Korean J. Ophthalmol.* **2020**, *34*, 75. [[CrossRef](#)]

18. Zhang, C.; Guo, Y.; Miller, N.R.; Bernstein, S.L. Optic nerve infarction and post-ischemic inflammation in the rodent model of anterior ischemic optic neuropathy (rAION). *Brain Res.* **2009**, *1264*, 67–75. [[CrossRef](#)]
19. Liu, P.-K.; Wen, Y.-T.; Lin, W.; Kapupara, K.; Tai, M.; Tsai, R.-K. Neuroprotective effects of low-dose G-CSF plus meloxicam in a rat model of anterior ischemic optic neuropathy. *Sci. Rep.* **2020**, *10*, 10351. [[CrossRef](#)]
20. Slater, B.; Vilson, F.L.; Guo, Y.; Weinreich, D.; Hwang, S.; Bernstein, S.L. Optic Nerve Inflammation and Demyelination in a Rodent Model of Nonarteritic Anterior Ischemic Optic Neuropathy. *Investig. Ophthalmol. Vis. Sci.* **2013**, *54*, 7952–7961. [[CrossRef](#)]
21. Lin, S.-F.; Chien, J.-Y.; Kapupara, K.; Huang, C.-Y.F.; Huang, S.-P. Oroxylin A promotes retinal ganglion cell survival in a rat optic nerve crush model. *PLoS ONE* **2017**, *12*, e0178584. [[CrossRef](#)]
22. Chen, Y.; Yang, L.; Lee, T.J. Oroxylin A inhibition of lipopolysaccharide-induced iNOS and COX-2 gene expression via suppression of nuclear factor-kappaB activation. *Biochem. Pharmacol.* **2000**, *59*, 1445–1457. [[CrossRef](#)]
23. Lee, J.Y.; Park, W. Anti-inflammatory effects of oroxylin A on RAW 264.7 mouse macrophages induced with polyinosinic-polycytidylic acid. *Exp. Ther. Med.* **2016**, *12*, 151–156. [[CrossRef](#)]
24. Li, J.; Tong, D.; Liu, J.; Chen, F.; Shen, Y. Oroxylin A attenuates cigarette smoke-induced lung inflammation by activating Nrf2. *Int. Immunopharmacol.* **2016**, *40*, 524–529. [[CrossRef](#)]
25. Ye, M.; Wang, Q.; Zhang, W.; Li, Z.; Wang, Y.; Hu, R. Oroxylin A exerts anti-inflammatory activity on lipopolysaccharide-induced mouse macrophage via Nrf2/ARE activation. *Biochem. Cell Biol.* **2014**, *92*, 337–348. [[CrossRef](#)]
26. Han, Q.; Wang, H.; Xiao, C.; Fu, B.-D.; Du, C.-T. Oroxylin A inhibits H₂O₂-induced oxidative stress in PC12 cells. *Nat. Prod. Res.* **2016**, *31*, 1339–1342. [[CrossRef](#)] [[PubMed](#)]
27. Ku, S.-K.; Lee, I.-C.; Bae, J.-S. Antithrombotic activities of oroxylin A in vitro and in vivo. *Arch. Pharmacol. Res.* **2013**, *37*, 679–686. [[CrossRef](#)]
28. Kim, D.H.; Jeon, S.J.; Son, K.H.; Jung, J.W.; Lee, S.; Yoon, B.H.; Lee, J.-J.; Cho, Y.-W.; Cheong, J.H.; Ko, K.H.; et al. The ameliorating effect of oroxylin A on scopolamine-induced memory impairment in mice. *Neurobiol. Learn. Mem.* **2007**, *87*, 536–546. [[CrossRef](#)] [[PubMed](#)]
29. Lee, S.; Kim, N.H.; Lee, N.H.; Jeon, S.J.; Lee, C.H.; Son, K.H.; Jung, J.W.; Shin, C.Y.; Ryu, J.H.; Oroxylin, A. A Flavonoid, Stimulates Adult Neurogenesis in the Hippocampal Dentate Gyrus Region of Mice. *Neurochem. Res.* **2010**, *35*, 1725–1732. [[CrossRef](#)] [[PubMed](#)]
30. Kim, D.H.; Jeon, S.J.; Son, K.H.; Jung, J.W.; Lee, S.; Yoon, B.H.; Choi, J.W.; Cheong, J.H.; Ko, K.H.; Ryu, J.H. Effect of the flavonoid, oroxylin A, on transient cerebral hypoperfusion-induced memory impairment in mice. *Pharmacol. Biochem. Behav.* **2006**, *85*, 658–668. [[CrossRef](#)]
31. Kim, D.H.; Kim, S.; Jeon, S.J.; Son, K.H.; Lee, S.; Yoon, B.H.; Cheong, J.H.; Ko, K.H.; Ryu, J.H. The effects of acute and repeated oroxylin A treatments on Aβ_{25–35}-induced memory impairment in mice. *Neuropharmacology* **2008**, *55*, 639–647. [[CrossRef](#)]
32. Kapupara, K.; Huang, T.-L.; Wen, Y.-T.; Huang, S.-P.; Tsai, R.-K. Optic nerve head width and retinal nerve fiber layer changes are proper indexes for validating the successful induction of experimental anterior ischemic optic neuropathy. *Exp. Eye Res.* **2019**, *181*, 105–111. [[CrossRef](#)] [[PubMed](#)]
33. Huang, S.P.; Chien, J.Y.; Tsai, R.K. Ethambutol induces impaired autophagic flux and apoptosis in the rat retina. *Dis. Model. Mech.* **2015**, *8*, 977–987. [[CrossRef](#)] [[PubMed](#)]
34. Chien, J.-Y.; Sheu, J.-H.; Wen, Z.-H.; Tsai, R.-K.; Huang, S.-P. Neuroprotective effect of 4-(Phenylsulfanyl)butan-2-one on optic nerve crush model in rats. *Exp. Eye Res.* **2016**, *143*, 148–157. [[CrossRef](#)]
35. Kambhampati, S.P.; Clunies-Ross, A.J.M.; Bhutto, I.; Mishra, M.K.; Edwards, M.; McLeod, D.S.; Kannan, R.M.; Luttly, G. Systemic and Intravitreal Delivery of Dendrimers to Activated Microglia/Macrophage in Ischemia/Reperfusion Mouse Retina. *Investig. Ophthalmol. Vis. Sci.* **2015**, *56*, 4413–4424. [[CrossRef](#)]
36. Cao, X.; Li, W.; Liu, Y.; Huang, H.; Ye, C.-H. The Anti-Inflammatory Effects of CXCR5 in the Mice Retina following Ischemia-Reperfusion Injury. *BioMed Res. Int.* **2019**, *2019*, 1–10. [[CrossRef](#)] [[PubMed](#)]
37. Avraham, B.C.R.; Dotan, G.; Hasanreisoglu, M.; Kramer, M.; Monselise, Y.; Cohen, Y.; Weinberger, V.; Goldenberg-Cohen, N. Increased Plasma and Optic Nerve Levels of IL-6, TNF-α, and MIP-2 Following Induction of Ischemic Optic Neuropathy in Mice. *Curr. Eye Res.* **2008**, *33*, 395–401. [[CrossRef](#)]
38. Sprinkle, T.J. 2',3'-cyclic nucleotide 3'-phosphodiesterase, an oligodendrocyte-Schwann cell and myelin-associated enzyme of the nervous system. *Crit. Rev. Neurobiol.* **1989**, *4*, 235–301. [[PubMed](#)]
39. Vlkolinský, R.; Cairns, N.; Fountoulakis, M.; Lubec, G. Decreased brain levels of 2',3'-cyclic nucleotide-3'-phosphodiesterase in Down syndrome and Alzheimer's disease. *Neurobiol. Aging* **2001**, *22*, 547–553. [[CrossRef](#)]
40. Göpfert, E.; Pytlík, S.; Debuch, H. 2',3'-Cyclic Nucleotide 3'-Phosphohydrolase and Lipids of Myelin from Multiple Sclerosis and Normal Brains. *J. Neurochem.* **1980**, *34*, 732–739. [[CrossRef](#)]
41. Lappe-Siefke, C.; Goebbels, S.; Gravel, M.; Nicksch, E.; Lee, J.; Braun, P.E.; Griffiths, I.R.; Nave, K.-A. Disruption of Cnp1 uncouples oligodendroglial functions in axonal support and myelination. *Nat. Genet.* **2003**, *33*, 366–374. [[CrossRef](#)] [[PubMed](#)]
42. Hagemeyer, N.; Goebbels, S.; Papiol, S.; Kästner, A.; Hofer, S.; Begemann, M.; Gerwig, U.C.; Boretius, S.; Wieser, G.L.; Ronnenberg, A.; et al. A myelin gene causative of a catatonia-depression syndrome upon aging. *EMBO Mol. Med.* **2012**, *4*, 528–539. [[CrossRef](#)] [[PubMed](#)]
43. Wu, W.; Gu, W.; Xu, X.; Shang, S.; Zhao, Z. Downregulation of CNPase in a MeCP2 deficient mouse model of Rett syndrome. *Neurol. Res.* **2012**, *34*, 107–113. [[CrossRef](#)]

44. Suda, H.; Hosokawa, T.; Ohno, R.; Hamaguchi, K.; Tsukada, Y. 2',3'-Cyclic nucleotide 3'-phosphodiesterase activity in the cerebrospinal fluid of patients with demyelinating diseases. *Neurochem. Pathol.* **1984**, *2*, 85–102. [[CrossRef](#)] [[PubMed](#)]
45. Yang, J.; Zhao, Y.; Zhang, L.; Fan, H.; Qi, C.; Zhang, K.; Liu, X.; Fei, L.; Chen, S.; Wang, M.; et al. RIPK3/MLKL-Mediated Neuronal Necroptosis Modulates the M1/M2 Polarization of Microglia/Macrophages in the Ischemic Cortex. *Cereb. Cortex* **2018**, *28*, 2622–2635. [[CrossRef](#)] [[PubMed](#)]
46. Lin, J.; Pan, X.; Huang, C.; Gu, M.; Chen, X.; Zheng, X.; Shao, Z.; Hu, S.; Wang, B.; Lin, H.; et al. Dual regulation of microglia and neurons by Astragaloside IV-mediated mTORC1 suppression promotes functional recovery after acute spinal cord injury. *J. Cell. Mol. Med.* **2020**, *24*, 671–685. [[CrossRef](#)]
47. Ni, J.; Wu, Z.; Peterts, C.; Yamamoto, K.; Qing, H.; Nakanishi, H. The Critical Role of Proteolytic Relay through Cathepsins B and E in the Phenotypic Change of Microglia/Macrophage. *J. Neurosci.* **2015**, *35*, 12488–12501. [[CrossRef](#)]
48. Salgado, C.; Vilson, F.; Miller, N.R.; Bernstein, S.L. Cellular inflammation in nonarteritic anterior ischemic optic neuropathy and its primate model. *Arch. Ophthalmol.* **2011**, *129*, 1583–1591. [[CrossRef](#)]
49. Tura, A.; Schuettauf, F.; Monnier, P.P.; Bartz-Schmidt, K.U.; Henke-Fahle, S. Efficacy of Rho-kinase Inhibition in Promoting Cell Survival and Reducing Reactive Gliosis in the Rodent Retina. *Investig. Ophthalmol. Vis. Sci.* **2009**, *50*, 452–461. [[CrossRef](#)]
50. Fisher, J.; Mizrahi, T.; Schori, H.; Yoles, E.; Levkovitch-Verbin, H.; Haggiag, S.; Revel, M.; Schwartz, M. Increased post-traumatic survival of neurons in IL-6-knockout mice on a background of EAE susceptibility. *J. Neuroimmunol.* **2001**, *119*, 1–9. [[CrossRef](#)]
51. Echevarria, F.D.; Formichella, C.R.; Sappington, R.M. Interleukin-6 Deficiency Attenuates Retinal Ganglion Cell Axonopathy and Glaucoma-Related Vision Loss. *Front. Neurosci.* **2017**, *11*, 318. [[CrossRef](#)]
52. Zahir-Jouzani, F.; Atyabi, F.; Mojtavavi, N. Interleukin-6 participation in pathology of ocular diseases. *Pathophysiology* **2017**, *24*, 123–131. [[CrossRef](#)]
53. Chidlow, G.; Wood, J.P.; Ebner, A.; Casson, R.J. Interleukin-6 is an efficacious marker of axonal transport disruption during experimental glaucoma and stimulates neuritegenesis in cultured retinal ganglion cells. *Neurobiol. Dis.* **2012**, *48*, 568–581. [[CrossRef](#)] [[PubMed](#)]
54. Argyropoulou, M.I.; Zikou, A.K.; Tzovara, I.; Nikas, A.; Blekas, K.; Margariti, P.; Galatsanos, N.; Asproudis, I. Non-arteritic anterior ischaemic optic neuropathy: Evaluation of the brain and optic pathway by conventional MRI and magnetisation transfer imaging. *Eur. Radiol.* **2006**, *17*, 1669–1674. [[CrossRef](#)] [[PubMed](#)]
55. Janáky, M.; Fülöp, Z.; Pálffy, A.; Benedek, K.; Benedek, G. Electrophysiological findings in patients with nonarteritic anterior ischemic optic neuropathy. *Clin. Neurophysiol.* **2006**, *117*, 1158–1166. [[CrossRef](#)] [[PubMed](#)]
56. Crain, J.M.; Nikodemova, M.; Watters, J.J. Microglia express distinct M1 and M2 phenotypic markers in the postnatal and adult central nervous system in male and female mice. *J. Neurosci. Res.* **2013**, *91*, 1143–1151. [[CrossRef](#)]
57. Cunha, C.; Gomes, C.; Vaz, A.R.; Brites, D. Exploring New Inflammatory Biomarkers and Pathways during LPS-Induced M1 Polarization. *Mediat. Inflamm.* **2016**, *2016*, 1–17. [[CrossRef](#)]
58. Tang, Y.; Le, W. Differential Roles of M1 and M2 Microglia in Neurodegenerative Diseases. *Mol. Neurobiol.* **2016**, *53*, 1181–1194. [[CrossRef](#)]
59. Xiao, L.; Zheng, H.; Li, J.; Wang, Q.; Sun, H. Neuroinflammation Mediated by NLRP3 Inflammasome After Intracerebral Hemorrhage and Potential Therapeutic Targets. *Mol. Neurobiol.* **2020**, *57*, 5130–5149. [[CrossRef](#)]
60. Henkel, J.S.; Beers, D.R.; Zhao, W.; Appel, S.H. Microglia in ALS: The Good, The Bad, and The Resting. *J. Neuroimmune Pharmacol.* **2009**, *4*, 389–398. [[CrossRef](#)]
61. Boche, D.; Perry, V.H.; Nicoll, J. Review: Activation patterns of microglia and their identification in the human brain. *Neuropathol. Appl. Neurobiol.* **2013**, *39*, 3–18. [[CrossRef](#)]
62. Franco, R.; Fernández-Suárez, D. Alternatively activated microglia and macrophages in the central nervous system. *Prog. Neurobiol.* **2015**, *131*, 65–86. [[CrossRef](#)]
63. Sabahi, M.; Joshaghanian, A.; Dolatshahi, M.; Jabbari, P.; Rahmani, F.; Rezaei, N. Modification of Glial Cell Activation through Dendritic Cell Vaccination: Promises for Treatment of Neurodegenerative Diseases. *J. Mol. Neurosci.* **2021**, 1–15. [[CrossRef](#)]
64. Kimura, A.; Namekata, K.; Guo, X.; Noro, T.; Harada, C.; Harada, T. Targeting Oxidative Stress for Treatment of Glaucoma and Optic Neuritis. *Oxidative Med. Cell. Longev.* **2017**, *2017*, 1–8. [[CrossRef](#)] [[PubMed](#)]
65. Williams, D.L. Oxidative Stress and the Eye. *Veter. Clin. North. Am. Small Anim. Pr.* **2008**, *38*, 179–192. [[CrossRef](#)] [[PubMed](#)]
66. Khan, R.S.; Fonseca-Kelly, Z.; Callinan, C.; Zuo, L.; Sachdeva, M.M.; Shindler, K.S. SIRT1 activating compounds reduce oxidative stress and prevent cell death in neuronal cells. *Front. Cell. Neurosci.* **2012**, *6*, 63. [[CrossRef](#)] [[PubMed](#)]
67. McDougald, D.S.; Dine, K.E.; Zezulin, A.U.; Bennett, J.; Shindler, K.S. SIRT1 and NRF2 Gene Transfer Mediate Distinct Neuroprotective Effects Upon Retinal Ganglion Cell Survival and Function in Experimental Optic Neuritis. *Investig. Ophthalmol. Vis. Sci.* **2018**, *59*, 1212–1220. [[CrossRef](#)]
68. Zhang, Y.; Xu, N.; Ding, Y.; Zhang, Y.; Li, Q.; Flores, J.; Haghighiabyaneh, M.; Doycheva, D.; Tang, J.; Zhang, J.H. Chemerin suppresses neuroinflammation and improves neurological recovery via CaMKK2/AMPK/Nrf2 pathway after germinal matrix hemorrhage in neonatal rats. *Brain, Behav. Immun.* **2018**, *70*, 179–193. [[CrossRef](#)]
69. Fujita, K.; Nishiguchi, K.M.; Shiga, Y.; Nakazawa, T. Spatially and Temporally Regulated NRF2 Gene Therapy Using Mcp-1 Promoter in Retinal Ganglion Cell Injury. *Mol. Ther. Methods Clin. Dev.* **2017**, *5*, 130–141. [[CrossRef](#)]
70. Larabee, C.M.; Desai, S.; Agasing, A.; Georgescu, C.; Wren, J.D.; Axtell, R.C.; Plafker, S.M. Loss of Nrf2 exacerbates the visual deficits and optic neuritis elicited by experimental autoimmune encephalomyelitis. *Mol. Vis.* **2016**, *22*, 1503–1513.

71. Yan, F.; Chen, S.H.; Li, X.J.; Nie, C.; Xie, H.N. Analysis of the activation of the Nrf2-ARE pathway following optic nerve injury in mice. *Eye Sci.* **2012**, *27*, 161–164. [[PubMed](#)]
72. Chen, F.; Hu, M.; Shen, Y.; Zhu, W.; Cao, A.; Ni, B.; Qian, J.; Yang, J. Isorhamnetin promotes functional recovery in rats with spinal cord injury by abating oxidative stress and modulating M2 macrophages/microglia polarization. *Eur. J. Pharmacol.* **2021**, *895*, 173878. [[CrossRef](#)] [[PubMed](#)]
73. Liao, S.; Wu, J.; Liu, R.; Wang, S.; Luo, J.; Yang, Y.; Qin, Y.; Li, T.; Zheng, X.; Song, J.; et al. A novel compound DBZ ameliorates neuroinflammation in LPS-stimulated microglia and ischemic stroke rats: Role of Akt(Ser473)/GSK3 β (Ser9)-mediated Nrf2 activation. *Redox Biol.* **2020**, *36*, 101644. [[CrossRef](#)] [[PubMed](#)]
74. Wang, Y.; Huang, Y.; Xu, Y.; Ruan, W.; Wang, H.; Zhang, Y.; Saavedra, J.M.; Zhang, L.; Huang, Z.; Pang, T. A Dual AMPK/Nrf2 Activator Reduces Brain Inflammation After Stroke by Enhancing Microglia M2 Polarization. *Antioxid. Redox Signal.* **2018**, *28*, 141–163. [[CrossRef](#)]
75. Chen, J.; Yin, W.; Tu, Y.; Wang, S.; Yang, X.; Chen, Q.; Zhang, X.; Han, Y.; Pi, R. L-F001, a novel multifunctional ROCK inhibitor, suppresses neuroinflammation in vitro and in vivo: Involvement of NF- κ B inhibition and Nrf2 pathway activation. *Eur. J. Pharmacol.* **2017**, *806*, 1–9. [[CrossRef](#)] [[PubMed](#)]
76. MacDowell, K.S.; Caso, J.R.; Martín-Hernández, D.; Moreno, B.M.; Madrigal, J.L.M.; Micó, J.A.; Leza, J.C.; García-Bueno, B. The Atypical Antipsychotic Paliperidone Regulates Endogenous Antioxidant/Anti-Inflammatory Pathways in Rat Models of Acute and Chronic Restraint Stress. *Neurotherapeutics* **2016**, *13*, 833–843. [[CrossRef](#)] [[PubMed](#)]